



# Design of a narrow band-pass birefringent filter for visible range

NILANJAN MUKHOPADHYAY<sup>1,\*</sup>, ARIJIT SAHA<sup>2</sup> and KALLOL BHATTACHARYA<sup>3</sup>

<sup>1</sup>Department of Electronics and Communication Engineering, Global Institute of Management and Technology, Krishnagar, Nadia 741 102, India

<sup>2</sup>Department of Electronics and Communication Engineering, B. P. Poddar Institute of Management and Technology, 137, VIP Road, Kolkata 700 052, India

<sup>3</sup>Department of Applied Optics and Photonics, University of Calcutta, JD-2, Sector 3, Salt Lake City, Kolkata 700 098, India

\*Corresponding author. E-mail: nilu.opt@gmail.com

MS received 27 December 2020; revised 1 April 2021; accepted 23 April 2021

**Abstract.** In this communication, the construction and transmission characteristics of a narrow band-pass birefringent filter have been investigated. The filter is formed by a combination of two sets of retarders with a polariser in between, and two linear polarisers placed at the two extreme ends. The sets of retarders are chosen to be a cascaded fan-type Solc filter having two different kinds of retardations, resulting in filtering characteristics better than those birefringent filters proposed for the visible range. The performance of this proposed filter is better in terms of effective suppression of side peak amplitudes as well as reduction of bandwidth with less number of waveplates. This birefringent filter can be used inside a linear resonator.

**Keywords.** Narrow band-pass birefringent filter; polariser; retarder; laser.

**PACS Nos** 42.79.Ci; 42.79.-e; 42.25.Lc

## 1. Introduction

The basic principle in birefringent filters is that light generating in a single polarisation state is made to interfere with itself. The concept of interference obtained in Michelson interferometer, i.e. by combining the rays travelling along different path lengths after being split from the input beam, is followed in a birefringent medium that is optically anisotropic to produce a relative phase delay between two orthogonal polarisations aligned along the fast and slow axes of the crystal. They are characterised to have very sharp transmission bands (down to a few nm in width). The transmission bands of a birefringent filter can be adjusted by different methods, including the use of elements of variable thickness, phase shifters etc. The electro-optical phase shifters are generally used in most of the applications with certain advantages. However, phase shifters composed of rotating wave plates are advantageous for specific applications, such as spectrophotometry. Birefringent filters are generally composed of one or several crystalline quartz plates. These filters find wide applications as tuning elements in dye lasers with advantages of high

dispersion, low loss and resistance to damage at high intensity. They can be designed with a series of perfect polarisers, partial polarisers, or only an entrance and an exit polariser. Based on design elements, primarily two types of optical filters exist, viz. active filters and passive filters. Active filters are based on electro-optic phenomena mainly designed by liquid crystals, while passive filters consist of components like birefringent plates, prism etc. The narrow band in the filter output is formed by the superposition of the polarised spectra produced by many retardation plates such as x-cut plate of quartz or other birefringent crystal, when placed between crossed or parallel polariser. Till date different types of birefringent filters have been reported, viz. the Lyot filter, the Solc filter, the Hurlbut filter, the mixed Solc filter and tunable liquid crystal filters to name a few. Among different applications, birefringent filters can be used for tuning lasers, with some advantages over other optical components like prisms, gratings etc. These filters can also be used for separation of different wavelength signals, dye laser tuning, line-narrowing in solid-state lasers, etc. Birefringent filter was first introduced by the French astronomer Lyot [1] in 1933, where

each retarder has twice the thickness compared to the preceding one. After nearly two decades, research in the domain of polarisation filters was restarted when the Czechoslovakian physicist, Solc introduced a second type of birefringent filter, which is today popularly known as the Solc filter, having a different construction than that of the Lyot filter. Solc filter [2–4] uses a series of  $n$  identical retarders arranged in such a way that,  $\theta = \pi/2n$ , where  $\theta$  is the angle between the principal directions of the successive retardation plates. In the year 1952, Hurlbut and Rosenfeld [5] showed that circular birefringence can also be utilised for making polarisation filters. The transmission of Solc filters was derived by Evans [6]. Billings [7] introduced an electro-optical tuning technique, achieved by changing the retardation of successive elements using Kerr cells. A modified Solc filter, the mixed Solc birefringent filter (MSBF), where the geometrical angle of orientation of individual retarders was affected by optical rotation, was proposed by Ghosh and Chakraborty [8]. The concept of classical fan-type Solc filter, where a stack of linearly twisted birefringent plates with arbitrary successive twist angles having total twist equals an odd integer of  $\pi/2$ , and each plate acts as a full wave plate was also proposed [9]. A mixed birefringent filter (MBF), where both circular birefringence and linear birefringence have been utilised in the fabrication, was introduced by Ghosh *et al* [10]. As the transmission characteristics of these types of filters are the same as that of the Solc filter, these filters are named as mixed birefringent Solc filters (MBSF). Hawkeye *et al* [11] proposed a narrow band-pass characteristic optical filter fabricated with one-dimensional periodic inhomogeneous thin films. But, glancing angle deposition technique is required to achieve the nanoscale precision to fabricate periodic gradient index thin films which is a bit complicated. In recent times, a composite birefringent filter (CBF) [12], where a cascaded system of two different sets of retarders having different values of retardations with two linear polarisers at both ends and one polariser at the middle of the two stacks has been reported. The bandwidth of this filter was about 14 nm using 10 plates with some significant secondary peaks. The bandwidth can be reduced by increasing the number of plates but that will lead to reflection loss. To suppress the secondary peak, a system [13] where glass plates are positioned at Brewster angle replacing the linear polarisers at both ends of the birefringent filter can be used. However, disadvantage of the system is its complex arrangement. In recent times, a different approach for Solc filter designing has been proposed using bulk anisotropic crystal [14]. But due to the elasto-optical effects on the surface of the crystal [15], the central wavelength will shift to longer or shorter wavelength

according to the direction and the value of the applied stress. Another method of designing an optical filter [16] that combines pigment-based colorant photorealist microlithography with traditional multilayer vacuum deposition technologies has been reported. However, the technique requires high level of precision and it is very costly too.

In the present article, the transmission characteristics of a narrow band-pass birefringent filter (NBBF) designed with less number of plates that results in significant reduction in bandwidth have been studied in the visible range. Jones calculus method has been used for transmission characteristics analysis and the well-known property of the unimodular Jones matrix is used for evaluating its  $N$ th power. The proposed system shows a much more efficient wavelength filtering than the Solc filter and other proposed birefringent filters in the visible range.

The rest of the paper is divided as follows. Section 2 deals with the construction of the proposed filter followed by the mathematical analysis related to the design of the filter using Jones calculus in §3. Simulation results and discussions for the proposed system are given in §4 and in the last section conclusion is drawn followed by references.

## 2. The proposed filter

Figure 1 represents the block diagram of the proposed narrow band-pass birefringent filter. It consists of two sets of retarders having different retardations, and each set is rotated at angles  $\theta, 2\theta, \dots, N\theta$ , which follows the fan-type Solc filter construction. There are two linear polarisers at both ends denoted by  $P(0)$  and  $P(\alpha)$  respectively, and one in between the two sets denoted by  $P(\pi/2)$ . Here  $P(0)$  and  $P(\pi/2)$  represent the orientation of transmission axes of the polarisers and it indicates that they are in crossed position. Also,  $\alpha$  denotes the angle of rotation of the exit polariser.  $E_i$  and  $E_o$  indicate the input and output light wave whose direction of propagation is shown by the arrow sign. In our proposed set-up, the first set consists of three plates having retardation  $8\lambda$ , and the second set consists of four plates having retardation  $12\lambda$ . The internal arrangement of the proposed filter design is shown in figure 2.

## 3. Mathematical analysis of the transmission function

The characteristics of the filter can be described on the basis of transmission function of the system. The derivation of the transmission function is obtained with the help of Jones calculus as mentioned earlier. In order to

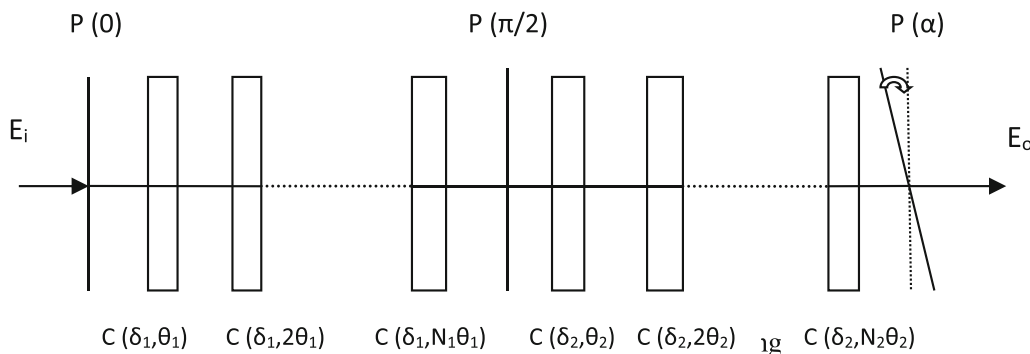


Figure 1. Block diagram of the proposed narrow band-pass birefringent filter.

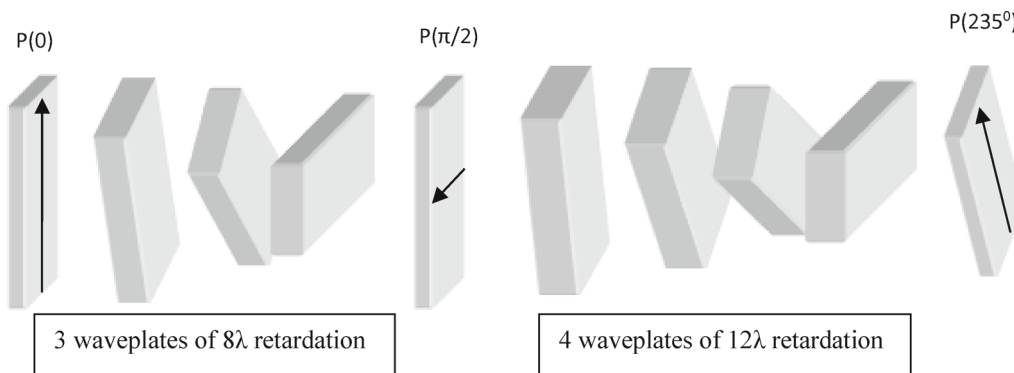


Figure 2. Schematic diagram for the internal arrangement of the proposed narrow band-pass birefringent filter.

obtain the transmission function of the proposed NBBF, the input beam is assumed to be represented by the Jones vector as

$$E_i = \begin{bmatrix} E_x \\ E_y \end{bmatrix}, \tag{1}$$

where  $E_x$  and  $E_y$  are the  $x$ -axis and  $y$ -axis components of the input beam. Initially, considering that the angle of the exit polariser is at  $0^\circ$ , i.e. transmission axis is parallel to that of the entrance polariser, the Jones vector of the beam emerging from the filter,  $E_o$ , may be written as

$$E_o = P(0)R(N_2\theta_2)[C(\delta_2)R(-\theta_2)]^{N_2} \times P\left(\frac{\pi}{2}\right)R(N_1\theta_1)[C(\delta_1)R(-\theta_1)]^{N_1}P(0)E_i, \tag{2}$$

where  $N_1$  is the number of retarders having retardation  $\delta_1$  and  $N_2$  is the number of retarders having retardation  $\delta_2$ ,  $P(\pi/2)$ ,  $P(0)$ ,  $C(\delta)$ ,  $R(-\theta_1)$  and  $R(-\theta_2)$  are the relevant Jones matrices of the elements of the filter given by

$$P(\alpha) = \begin{bmatrix} \cos^2 \alpha & \sin \alpha \cos \alpha \\ \sin \alpha \cos \alpha & \sin^2 \alpha \end{bmatrix}, \tag{3}$$

$$C(\delta) = \begin{bmatrix} \exp(i\delta/2) & 0 \\ 0 & \exp(-i\delta/2) \end{bmatrix} \tag{4}$$

and

$$R(-\theta) = \begin{bmatrix} \cos \theta & \sin \theta \\ -\sin \theta & \cos \theta \end{bmatrix}. \tag{5}$$

Let us assume

$$\begin{aligned} C(\delta_1)R(-\theta_1) &= M(\delta_1, \theta_1) \\ C(\delta_2)R(-\theta_2) &= M(\delta_2, \theta_2). \end{aligned} \tag{6}$$

Considering the fact that  $R(N_1\theta_1)$  and  $R(N_2\theta_2)$  are two unimodular matrices, the Jones vector of the outcoming beam according to eq. (2) may be written as

$$E_o = P(0)[M(\delta_2, \theta_2)]^{N_2} \times P\left(\frac{\pi}{2}\right)[M(\delta_1, \theta_1)]^{N_1}P(0)E_i. \tag{7}$$

Carrying out the matrix multiplications,  $M(\delta_1, \theta_1)$  and  $M(\delta_2, \theta_2)$  are found to be two unimodular matrices and the general expression is given by

$$M(\delta, \theta) = \begin{bmatrix} \cos \theta \exp(i\delta/2) & \exp(i\delta/2)\sin \theta \\ -\sin \theta \exp(-i\delta/2) & \cos \theta \exp(-i\delta/2) \end{bmatrix} \tag{8}$$

or in another way,

$$M(\delta, \theta) = \begin{bmatrix} m_{11} & m_{12} \\ m_{21} & m_{22} \end{bmatrix}. \tag{9}$$

We raise the matrix  $M(\delta_1, \theta_1)$  to the  $N_1$ th power. For this purpose, we make use of a well-known property of a unimodular matrix and we obtain

$$[M(\delta_1, \theta_1)]^{N_1} = \begin{bmatrix} m_{11}P_{N_1-1}(x_1) - P_{N_1-2}(x_1) & m_{12}P_{N_1-1}(x_1) \\ m_{21}P_{N_1-1}(x_1) & m_{22}P_{N_1-1}(x_1) - P_{N_1-2}(x_1) \end{bmatrix}, \tag{10}$$

where  $m_{ij}$  is the element in the  $i$ th row and  $j$ th column of the matrix  $M(\delta_1, \theta_1)$ , and assume

$$\begin{aligned} x_1 &= (m_{11} + m_{22})/2 = \cos \theta_1 \cos \delta_1/2 = \cos \phi_1 \\ \phi_1 &= \cos^{-1} x_1 \end{aligned} \tag{11}$$

and

$$(1 - x_1^2)^{\frac{1}{2}} = \sin \phi_1 \tag{12}$$

Similarly, when the matrix  $M(\delta_2, \theta_2)$  is raised to the  $N_2$ th power, we get

$$[M(\delta_2, \theta_2)]^{N_2} = \begin{bmatrix} m_{11}P_{N_2-1}(x_2) - P_{N_2-2}(x_2) & m_{12}P_{N_2-1}(x_2) \\ m_{21}P_{N_2-1}(x_2) & m_{22}P_{N_2-1}(x_2) - P_{N_2-2}(x_2) \end{bmatrix}, \tag{13}$$

where  $m_{ij}$  is the element in the  $i$ th row and  $j$ th column of the matrix  $M(\delta_2, \theta_2)$ , and assume

$$x_2 = (m_{11} + m_{22})/2 = \cos \theta_2 \cos \delta_2/2 = \cos \phi_2 \tag{14}$$

$$\phi_2 = \cos^{-1} x_2 \text{ and } (1 - x_2^2)^{\frac{1}{2}} = \sin \phi_2. \tag{15}$$

Here,  $P_N$ s are the Chebyshev polynomials of the second kind, given by

$$P_N(x) = \sin(N + 1) \cos^{-1} x / (1 - x^2)^{\frac{1}{2}}. \tag{16}$$

A proof of the above relation, based on the theory of matrices, was given by Abeles [17]. After performing the product operations on the right-hand side of eq. (7) the output beam may be written as

$$E_o = \begin{bmatrix} z \\ 0 \end{bmatrix} E_x, \tag{17}$$

where

$$\begin{aligned} z &= [(\sin \theta_2 \sin N_2 \phi_2 / \sin \phi_2) \exp(i\delta_2/2)] \\ &\times [(-\sin \theta_1 \sin N_1 \phi_1 / \sin \phi_1) \exp(-i\delta_1/2)]. \end{aligned} \tag{18}$$

Now the intensity transmittance of the filter  $T_0$ , when the two end polarisers are parallel is given by

$$T_0 = |z|^2 = \left| \frac{\sin(\theta_1)\sin(\theta_2)\sin(N_1\phi_1)\sin(N_2\phi_2}{\sin(\phi_1)\sin(\phi_2)} \right|^2. \tag{19}$$

If only one type of retarder with rotators in between two successive retarders are considered instead of two different types, the expression for the transmittance becomes identical to that of the MSBF reported in [8].

When the exit polariser is rotated by an angle  $\alpha$  then the Jones vector of the beam emerging from the filter,  $E_o$ , in eq. (2) may, therefore, be written as

$$\begin{aligned} E'_o &= P(\alpha)R(N_2\theta_2)[C(\delta_2)R(-\theta_2)]^{N_2} \\ &\times P\left(\frac{\pi}{2}\right)R(N_1\theta_1)[C(\delta_1)R(-\theta_1)]^{N_1}P(0)E_i, \end{aligned} \tag{20}$$

where the Jones vector for  $P(\alpha)$  is given by eq. (3). Now following similar calculations referred in eq. (7) to eq. (16) the output beam may be written as

$$E'_o = \begin{bmatrix} z_1 \\ z_2 \end{bmatrix} E_x, \tag{21}$$

where

$$\begin{aligned} z_1 &= [\cos^2\alpha m_{12}P_{N_2-1}(x_2) + \sin\alpha \cos\alpha (m_{22}P_{N_2-1}(x_2) \\ &\quad - P_{N_2-2}(x_2))] [m_{21}P_{N_1-1}(x_1)] \\ z_2 &= [\sin\alpha \cos\alpha m_{12}P_{N_2-1}(x_2) + \sin^2\alpha (m_{22}P_{N_2-1}(x_2) \\ &\quad - P_{N_2-2}(x_2))] [m_{21}P_{N_1-1}(x_1)]. \end{aligned} \tag{22}$$

So, the intensity transmittance of the filter,  $T'_0$ , when the exit polariser is rotated, can be given by

$$T'_0 = |(z_1 + z_2)|^2. \tag{23}$$

From eq. (23) overall transmission characteristics of the filter can be studied with the rotation of the transmission axis of the exit polariser.

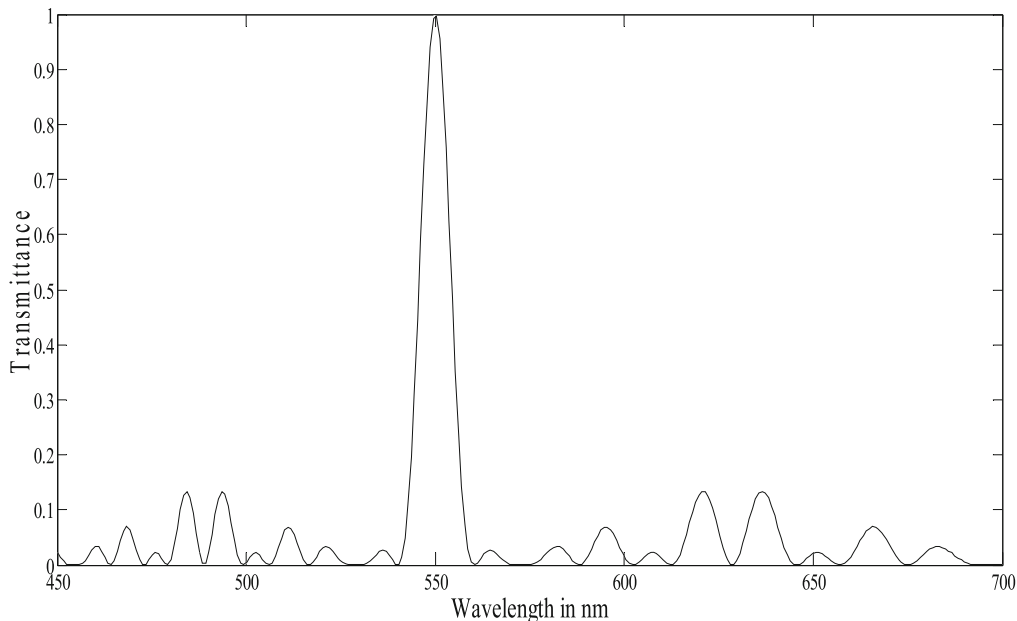


**Figure 3.** Transmission characteristics for the proposed NBBF with the exit and entrance polarisers in parallel position.

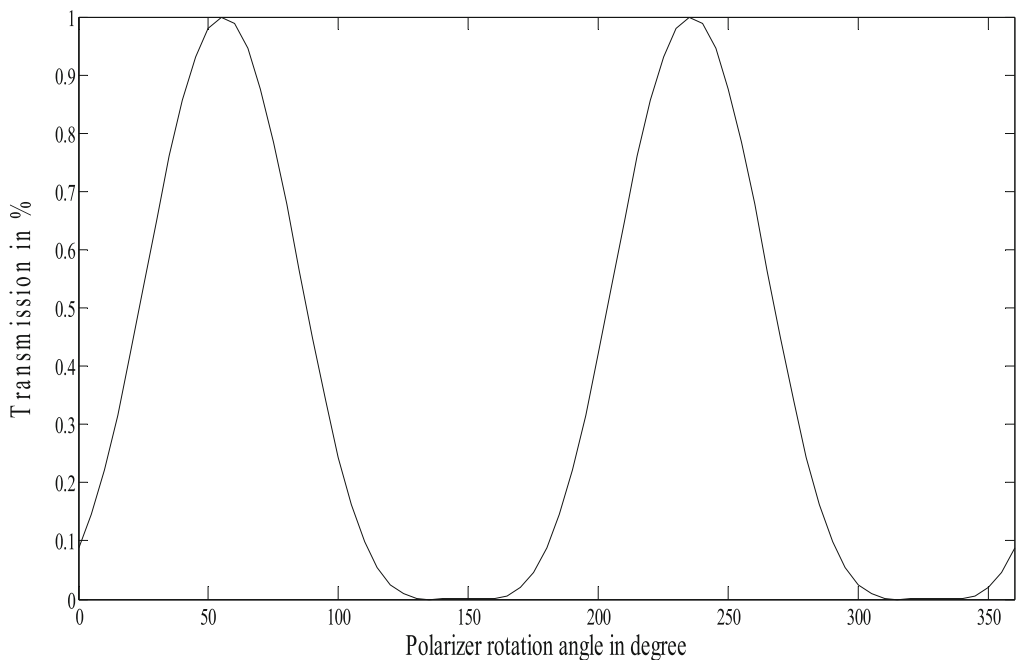


**Figure 4.** Variation of transmittance with the rotation angle of the exit polariser.

**4. Simulation results and discussion**

To study the transmission characteristics of the proposed filter, computation of the transmission function depending on the wavelength and the rotational angle of the polariser has been performed. The phase retardation introduced by the birefringent plates has to be taken under consideration and it is given by

$$\delta = \frac{2\pi}{\lambda_0}(n_e - n_o)d, \tag{24}$$

where  $d$  is the thickness of each plate,  $(n_e - n_o)$  is the birefringence of the material of the retarders and  $\lambda_0$  is the wavelength of light. Birefringence depends on wavelength, but it can be assumed that within the range of wavelengths under consideration, the birefringence

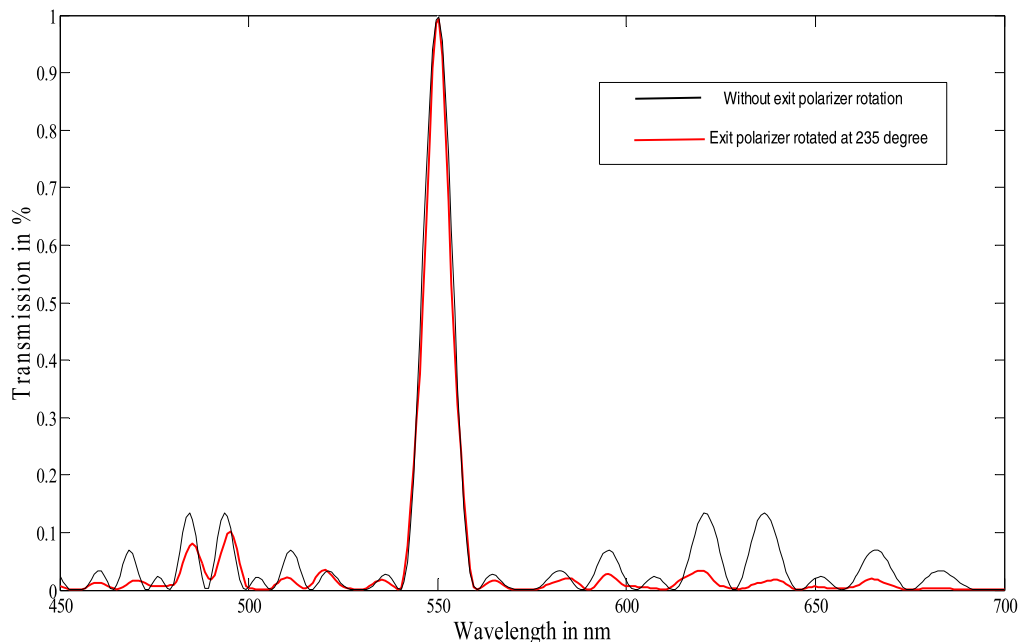


**Figure 5.** Comparison of transmission curve for the proposed filter with exit polariser rotated at 235° angle (black curve) and that for the polariser without rotation (red curve).

$(n_e - n_o)$  is constant. In that case we may write

$$\delta = \frac{D}{\lambda_0}, \tag{25}$$

where  $D$  is a constant.

The two sets of retarders, which follow the fan-type Solc filter construction with different numbers of waveplates, are rotated with different values, i.e.  $\theta_1$  and  $\theta_2$ . These values are chosen to satisfy the following conditions:

$$N_1\theta_1 = \frac{\pi}{2} \quad \text{and} \quad N_2\theta_2 = \frac{\pi}{2},$$

as stipulated by Evans [6]. In order to compute the transmittance of NBBF, the values of  $\theta_1$  and  $\theta_2$  are calculated in such a way that the above condition holds for the wavelength at which the peak transmission is desired.

All the simulations have been performed using MATLAB 2009a in a laptop with 2 GB RAM, Dual Core processor and Windows7 operating system. Figure 3 shows the transmission curve for the proposed NBBF, where three plates (i.e.  $N_1$ ) having retardation  $8\lambda$  and four plates (i.e.  $N_2$ ) having retardation  $12\lambda$  are used. In this case, the transmission axis of the exit polariser is parallel to that of the entrance polariser. The transmission curve shows a peak centred at 550 nm with some secondary peaks having significant amplitude over 600 nm on the right side and around 500 nm on the left side of the primary peak. After passing the exit polariser, the wavelength component at 550 nm is filtered out from

the incoming light wave and the rest of the wavelengths are suppressed due to the reduction in amplitude. Also the filter bandwidth is 5.1 nm which shows a significant improvement over the previously reported designs in the particular wavelength range.

Now we have rotated the transmission axis of the exit polariser, i.e. introduced a variation in rotation angle ( $\alpha$ ), and in effect the amplitudes of the secondary peaks start changing. So the amplitudes of the unwanted secondary peaks can be controlled by rotating the exit polariser at a suitable angle. Study of the dependency of transmission function on the rotation angle of the exit polariser is represented in figure 4 from which we can find a suitable angle. The simulation is performed using eq. (23). From the obtained result it can be observed that there are two angles of rotation, i.e., 55° and 235°, where the transmittance is maximum.

After obtaining the rotation angles we have studied the effect of rotation on the overall transmission characteristics of the filter. Figures 5 and 6 represent variation of the transmission function over 450–700 nm wavelength range for the rotation of transmission axis of the exit polariser at angles 235° and 55° respectively. Also both the results are compared with the result obtained when the exit polariser was parallel to the entrance polariser.

It is observed that amplitudes of secondary peaks are reduced on both sides of the primary peak centred at 550 nm. But at 235° rotational angle, that reduction in amplitude is significant and also the transmittance is maximum without much change in the bandwidth as

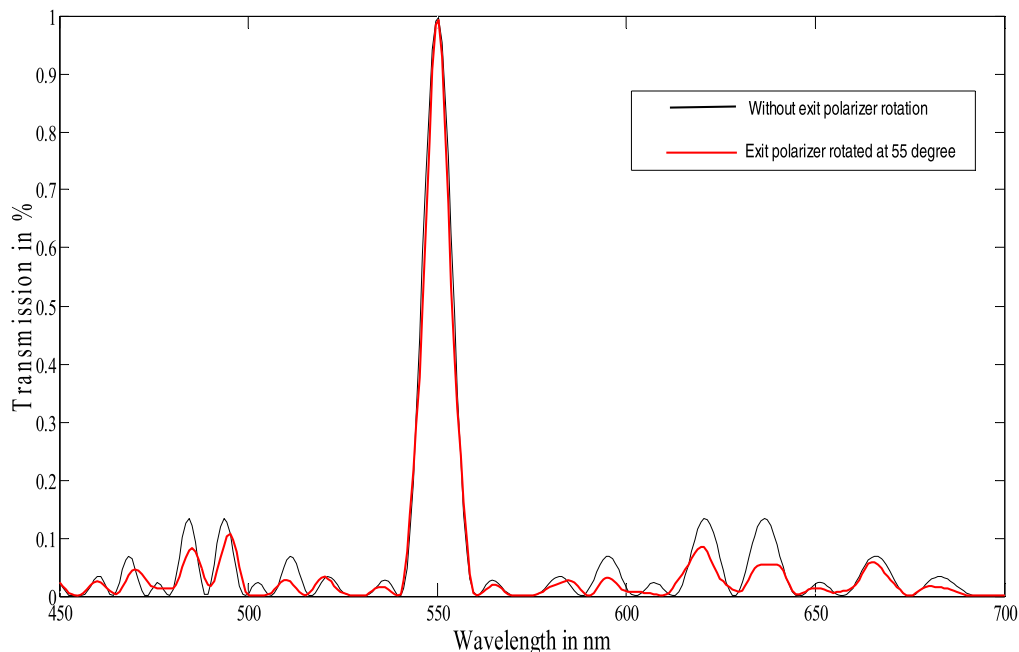


**Figure 6.** Comparison of transmission curve for the proposed filter with exit polariser rotated at 55° angle (black curve) and that for polariser without rotation (red curve).

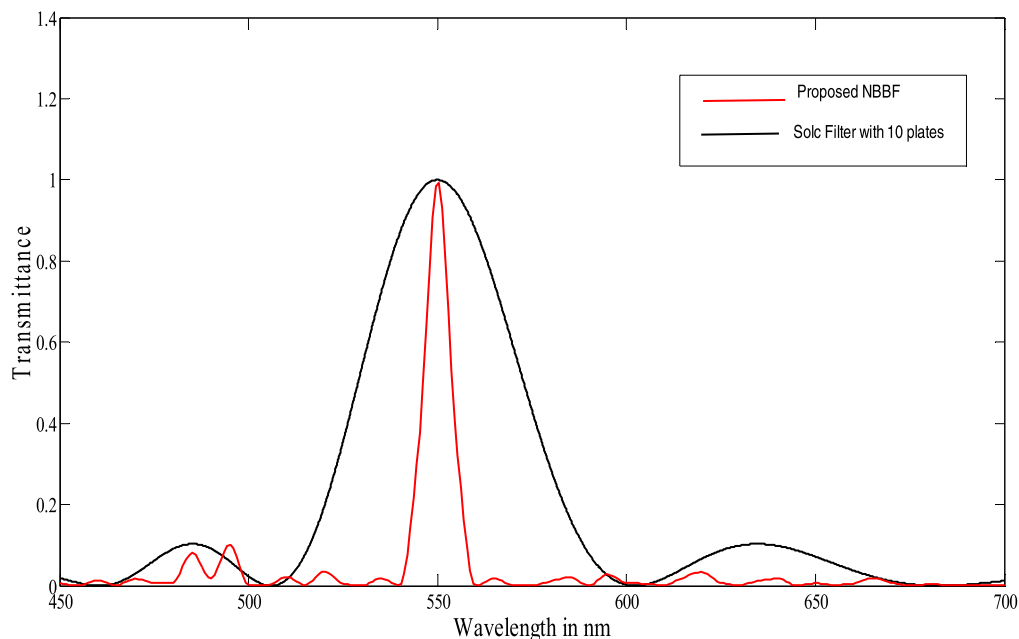


**Figure 7.** Comparison of transmission curve for the proposed filter with the exit polariser rotated at 235° angle (red curve) and that for the filter of [6] with crossed polariser (black curve).

obtained previously, i.e., around 5.1 nm. The rotation of the exit polariser affects only the amplitudes of the secondary peaks.

Therefore, our proposed birefringent filter set-up shows improvement in terms of reduction in bandwidth and secondary peaks as well. We have compared the obtained results with that of the other filters reported

in that particular wavelength range. Birefringent filter has wave plates of identical retardation type introduced by Evans [6], where ten plates of  $\lambda$  retardation were used. Figure 7 shows the comparison of the transmission curve of the proposed NBBF and that of the Solc filter. In the case of Solc filter, ten waveplates of identical retardation, i.e.  $\lambda$  were used. So, all the plates

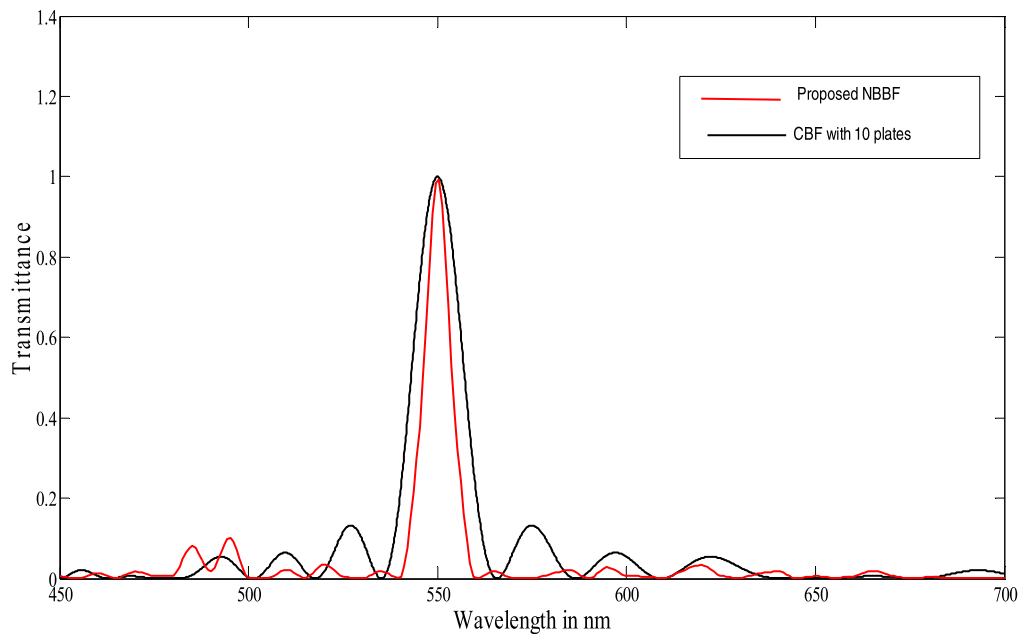


**Figure 8.** Comparison of transmission curve for the proposed filter with the exit polariser rotated at  $235^\circ$  angle (red curve) and that for the CBF (black curve).

have the same thickness. Also, the two polarisers, i.e. entrance and exit, were arranged in crossed position in the case of Solc filter. In our proposed filter, two stacks of waveplates having different retardations are used. The first stack contains three waveplates of  $8\lambda$  retardation and the second stack contains four waveplates of  $12\lambda$  retardation. So, the two stacks have waveplates of two different thicknesses and separated by a polariser having transmission axis rotated at  $90^\circ$  angle with respect to the input polariser. The exit polariser is at an angle of  $235^\circ$  with entrance polariser in our case whereas they were in crossed position in the Solc filter.

As the numbers of elements are reduced from that of the Solc filter, the experimental set-up of the proposed filter will be simpler. Also, in our proposed set-up, thicknesses of all the waveplates are greater than that of the Solc filter which will be helpful in the fabrication and mounting of the waveplates. From the comparison between two transmission curves we observed that there is a significant amount of reduction in half width, as well as side-peak amplitudes over the previous filter.

Figure 8 represents the comparison of the transmission curve of the proposed NBBF and that of the CBF reported earlier. The exit polariser is rotated at  $235^\circ$  angle in our proposed birefringent filter, whereas the entrance and exit polarisers were kept parallel in the CBF. The black curve in figure 8 shows the transmission

curve for CBF, where 10 plates of different retardations were used.

The red curve represents the transmission curve for our proposed NBBF, where we have used only 7 plates among which three plates (i.e.  $N_1$ ) have  $8\lambda$  retardation and four plates (i.e.  $N_2$ ) have  $12\lambda$  retardation. From this comparison plot it is clear that there is a significant improvement in the transmission characteristics in our proposed filter over the previous filter in terms of many aspects. Firstly, the full-width at half-maximum (FWHM) is reduced by a significant amount, i.e. in our case it is 5.1 nm over the previous reported value of around 14 nm. Secondly, the amplitudes of the side peaks are also reduced by a noticeable amount by rotating the exit polariser. In the case of our proposed NBBF, thicknesses of the plates are significant as they have higher retardation which will reduce the manufacturing complexity too. The half-width or bandwidth of the filter can be further reduced by increasing the number of plates but that will lead to reflection losses. In our proposed system, we achieved that goal with less number of plates having reduced reflection loss. Overall, reflection loss for the polarised input light is calculated to be 6.8% considering the entrance and exit reflection losses. Also, the calculated absorption loss is 7.5% along with internal reflection loss which is considered to be around 1% that in turn increases the overall transmission to 84.7% at 550 nm. Existing birefringent filters available in this wavelength range have transmission around 70–80%,

indicating an improvement of the proposed filter performance in terms of reflection loss.

## 5. Conclusion

A narrow band-pass birefringent filter having reduced number of plates which follows the fan-type Solc filter construction over 450–700 nm range has been presented where the transmission axis of the exit polariser is rotated at 235°. The transmission characteristics of the proposed filter suggest that it can pass a narrow band (i.e. 5.1 nm) centred at 550 nm and has reduced amplitude of secondary side peaks. The obtained results indicate a significant improvement of the performance over the previously reported filters in that particular wavelength range. The design is cost-effective as the number of plates gets reduced and also results in reduced manufacturing complexity compared to that of the previously reported CBF as well as thin film based systems. The loss due to reflections at the interfaces may be a major drawback of the system. This can be reduced by using a suitable antireflection coating on the faces of the plates. But, it can be immersed in a liquid having the same refractive index which may be a cheaper way. This birefringence-based optical filter may find potential applications in tuning dye lasers for achieving a narrow band and also in other optical applications in the intended wavelength range.

## References

- [1] L B Lyot, *C. R. Acad. Sci. (Paris)* **197**, 1593 (1933)
- [2] I Sole, *J. Opt Soc. Am.* **55**, 621 (1965)
- [3] I Sole, *Czech. J. Phys.* **4**, 53 (1954)
- [4] I Sole, *Czech. J. Phys.* **5**, 80 (1955)
- [5] C S Hurlbut and J L Rosenfeld, *J. Am. Mineral.* **37**, 158 (1952)
- [6] John W Evans, *J. Opt. Soc. Am.* **48**, 142 (1958)
- [7] Bruce H Billings, *J. Opt. Soc. Am.* **37**, 738 (1947)
- [8] A Ghosh and A K Chakraborty, *Opt. Acta: Int. J. Opt.* **29(10)**, 1407 (1982), <https://doi.org/10.1080/713820752>
- [9] I Abdulhalim, *Opt. Commun.* **267**, 36 (2006)
- [10] A Ghosh, J Basu and A K Chakraborty, *Opt. Laser Technol.* **18**, 23 (1986)
- [11] M M Hawkeye and M J Brett, *J. Appl. Phys.* **100**, 044322 (2016), <https://doi.org/10.1063/1.2335397>
- [12] A Saha, K Bhattacharya and A K Chakraborty, *J. Mod. Opt.* **56(8)**, 963 (2009)
- [13] G Holtom and O Teschke, *IEEE J. Quantum Electron.* **10(8)**, 577 (1974), <https://doi.org/10.1109/JQE.1974.1068208>
- [14] P Dey, A Dash and A Saha, *Optik* **127(22)**, 10366 (2016)
- [15] H Han *et al*, *Opt. Quant. Electron.* **50**, 28 (2018), <https://doi.org/10.1007/s11082-017-1289-8>
- [16] Jin Jian *et al*, *Applied mechanics and materials* (Trans Tech Publications, Ltd., 2013) Vol. 289, pp. 63–68, Crossref. <https://doi.org/10.4028/www.scientific.net/amm.289.63>
- [17] F Abeles, *Ann. Phys.* **12(5)**, 596 (1950), <https://doi.org/10.1051/anphys/195012050596>